2024 EAGE ANNUAL 85TH CONFERENCE & EXHIBITION OSLO | NORWAY

New geological understanding with land FWI Imaging, a Sultanate of Oman case study

Y. Guo[1], A. Aziz[1]

[1] CGG

Summary

Land FWI has been applied to seismic data in the Sultanate of Oman in the past years, but its usage has been limited to low frequency updates and input for migration purpose only. With proper input data conditioning, initial model preparation and velocity inversion, we have managed to run acoustic FWI to 35 Hz. An FWI Image was then derived from the velocity, producing a superior image of the complex fault system compared to the conventional methods due to the utilization of the full wavefield and the least square fitting from low to high frequencies.

New geological understanding with land FWI Imaging, a Sultanate of Oman case study

Introduction

Land seismic acquisition in the Sultanate of Oman has adopted several technological improvements in recent years. For example: low-frequency vibrators starting from 1.5 Hz (Mahrooqi et al., 2012, Baeten et al., 2013) improve low-frequency content compared to conventional vibrators starting from 6 or 8 Hz; and high-density nodal geophones not only increase the signal-to-noise ratio (SNR) but also record longer offsets with continuous recording (Zhao et al., 2018). These technologies provide better seismic input for full-waveform inversion (FWI).

Despite these improvements in recorded data, FWI still struggles with several challenges in this region. Firstly, whilst the high density and high fold acquisition improves the stack image, single node traces have more noise compared to the conventional geophone group. Simultaneous shooting also adds interference noise that particularly affects low-frequency SNR, where the blended noise appears coherent. Secondly, ground roll dominates the low-frequency energy where diving waves are very weak. Finally, a geologically complex and heterogeneous near surface not only generates strong noise, but also makes near-surface velocity estimation particularly challenging.

One of the early FWI trials in Oman was illustrated by Stopin et al. (2014). The FWI used diving waves, and the result showed good long-wavelength velocity update. Later on, Multi-Wave Inversion (MWI) followed by diving-wave FWI (Farooqui et al., 2021) further improved the shallow velocity resolution. Geological horizons were then better interpreted and used in tomography to update a structurally conformal velocity. An attempt at high-frequency FWI was presented by Hermant et al. (2020). The velocity was initially inverted with only diving waves up to 9 Hz, and then with cleanly processed reflections to 16 Hz. The first step updated the background velocity and then the reflections added details. However, high-frequency diving waves still contribute to middle- to short-wavelength velocity updates, so this flow is not suitable to push FWI to higher frequencies due to the disconnection between diving waves and reflections.

While still challenging for land data, successful applications of FWI with marine data, even in geologically complex regions, are well established (Wang et al., 2019). In particular, good examples of high-frequency FWI and FWI Imaging are achieved in both shallow and deep water regions, solving various geological challenges (Huang et al., 2021; Espin et al., 2023). These advances towards high-frequency FWI Imaging can be applied to land data with proper data preparation and handling of the velocity inversion.

Context and data preparation

The study area lies in the gravel plain of north Sultanate of Oman. The data was acquired in 2022 with vibrators of 1.5-86 Hz sweep frequency and simultaneous shooting with 25 m by 25 m shot spacing and 75 m by 100 m geophone node spacing. It has wide-azimuth coverage with maximum offset of about 13 km.

One of the exploration targets is the regional fault-related structures and reservoirs. The legacy result failed to resolve the horizontal and vertical velocity contrasts. Encouraged by the marine FWI Imaging successes and benefits in terms of sharp faulting resolution, we have implemented FWI Imaging in this land data case study.

After deblending, the low-frequency signal (1-6 Hz) was still fairly noisy (Figure 1), only enabling identification of the ground roll. This was the only coherent signal visible at this stage, with diving and reflected waves being much weaker and hidden behind ambient noise. Acoustic FWI was chosen for high-frequency FWI Imaging, so the ground roll needed to be removed. Matching pursuit linear Radon surface wave attenuation was applied to handle the strong ground roll and was followed by a four-dimension joint low-rank and sparse inversion (Sternfels et al., 2015) to attenuate the random noise. All the diving and reflected waves are then kept for use in FWI without any data muting.

High-frequency FWI Image result and discussion

The first challenge was the near-surface velocity. Acoustic FWI showed fast velocity leakage at about 100 m depth because the legacy near-surface velocity derived by refraction tomography was too fast, as shown in Figure 2. MWI makes use of ground roll dispersion curves and first breaks to build a better initial velocity (Bardainne, 2018; Masclet et al., 2019). FWI converged better with this improved near-surface velocity, showing a more geologically consistent update.

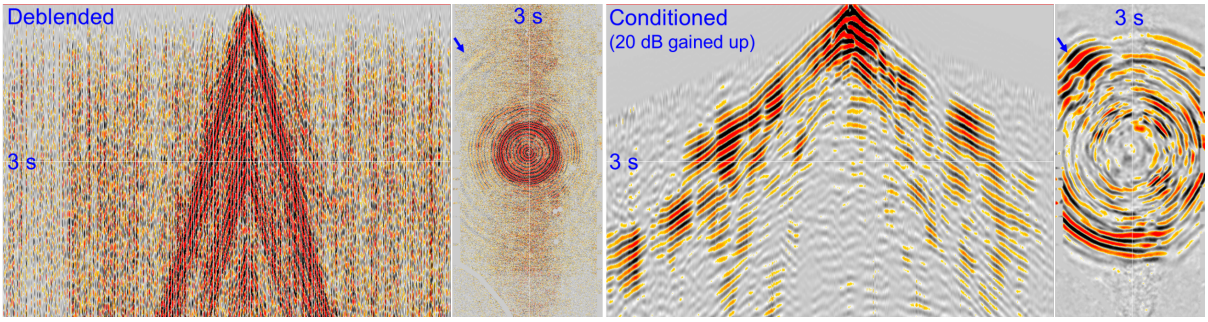

Figure 1. *Left: receiver gather 1-6 Hz and time slice at 3 seconds. Right: data after ground roll and random noise attenuation. Both are displayed in same size.*

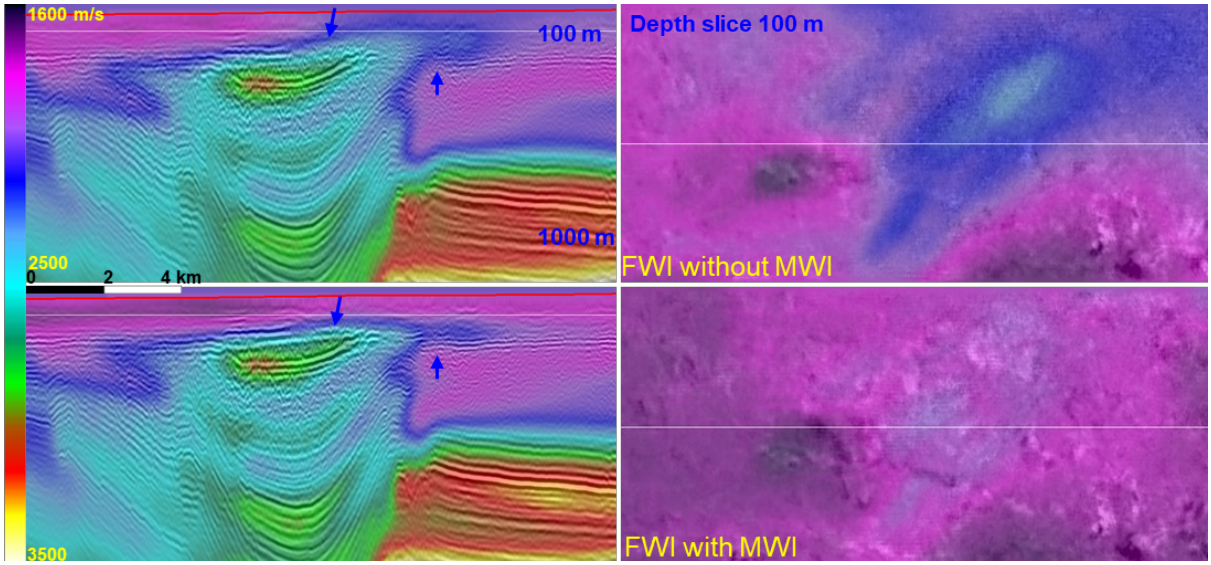

Figure 2. *Top: 6 Hz FWI velocity without MWI overlaid on Kirchhoff PSDM stack. Bottom: MWI for shallow 200 m followed by 6 Hz FWI update.*

Direct arrival energy is normally much weaker in recorded data than in synthetic modelling due to near-surface absorption. FWI with shallow attenuation (Wang et al., 2021) reduces the direct arrival energy in synthetic data and better matches recorded data. A free surface boundary condition is employed due to observable multiples in the recorded data.

Acoustic FWI inverted for velocities up to 35 Hz, and an FWI Image was created from the velocity model, assuming slowly varying density (Zhang et al., 2020), as shown in Figure 3.

The legacy velocity captured the background velocity trend, but the resolution was not sufficient to obtain a good migration image. FWI using the full data captures both vertical and horizontal velocity variations in the resulting model. With such detailed velocity, Kirchhoff migration gives an improved image except at the major fault where a sharp velocity contrast exists. RTM better handles the velocity contrast, but it is still limited by the use of primary reflections only. FWI Imaging makes use of the full wavefield and has low to high frequency iterative updates to explain the recorded data. Thus, it improves the complex fault imaging from shallow to deep and produces richer low-frequency content due to the kinematic background velocity update.

Although a good FWI Image was achieved, acoustic FWI seems unable to correct the very shallow velocity error. This could be due to the inaccurate physics of the near-surface modelling. Ground roll is the strongest energy in land data of Oman, reaching up to 95% of the recorded energy. While often treated as noise during processing, it contains useful near-surface information. MWI is limited by the use of ground roll dispersion curves instead of using the full waveform information, and the dispersion curve modeling is only 1D. Therefore, elastic FWI with ground roll can be considered as a better choice. This was explored by Leblanc et al. (2022) with virtual data built by interferometry using continuous recording and by Adwani et al. (2022) by inverting surface waves from active deblended data. With both virtual and active data, elastic FWI could potentially invert near-surface shear wave velocity and guide the P-wave velocity update. However, due to the intensive compute power needed, acoustic FWI will likely still be used to obtain the high-frequency FWI Image in the near future.

Conclusion

With proper handling of the input data conditioning and velocity inversion, we were able to obtain a stable, high-frequency velocity model and a corresponding FWI Image that improves the geological understanding of the faulted structures and reduces the exploration uncertainties in this study area from the north of the Sultanate of Oman. As the way forward, elastic FWI may invert for a more accurate near-surface velocity, and FWI Imaging is expected to gradually replace the structural stack, which often depends on complicated processing flows.

Acknowledgements

We thank Petroleum Development Oman and the Ministry of Energy and Minerals of the Sultanate of Oman for the permission to publish the data examples, and CGG for the permission to publish this work.

References

Adwani, A., Danilouchkine, M., Al-Siyabi, Q., Al-Droushi, O., Ten Kroode, F., Plessix, R. and Ernst, F. [2022] Onshore model building using elastic full-waveform inversion on surface and body waves: A case study from Sultanate of Oman. *Geophysics*, **87**(6), R413-R424.

Baeten, G., Maag, J., Plessix, R., Klaassen, R., Qureshi, T., Kleemeyer, M., Ten Kroode, F. and Rujie, Z. [2013] The use of low frequencies in a full-waveform inversion and impedance inversion land seismic case study. *Geophysical Prospecting*, **61**, 701–711.

Bardainne, T. [2018] Joint inversion of refracted P-waves, surface waves and reflectivity. *80th EAGE Conference & Exhibition*, Extended Abstracts, We-K-02.

Espin, I., Salaun, N., Jiang, H. and Reinier, M. [2023] From FWI to ultra-high-resolution imaging. *The Leading Edge*, **42**(1), 16-23.

Farooqui, M. S., Carotti, D. and Al-Jahdhami, M. [2021] Integrated high-resolution model building: a case study from the Sultanate of Oman. *82nd EAGE Conference & Exhibition*, Extended Abstracts.

Hermant, O., Aziz, A., Warzocha, S. and Al Jahdhami, M. [2020] Imaging complex fault structures on-shore Oman using optimal transport full waveform inversion. *82nd EAGE Conference & Exhibition*, Extended Abstracts.

Huang, R., Zhang Z., Wu Z., Wei Z., Mei J. and Wang P. [2021] Full-waveform inversion for full-wavefield imaging: Decades in the making. *The Leading Edge*, **40**(5), 324–334.

Leblanc, O., Sedova, A., Lambaré, G., Allemand, T., Hermant, O., Carotti, D., Donno, D. and Masmoudi, N. [2022] Elastic Land Full-Waveform Inversion in The Middle East: Method and Applications. *83rd EAGE Conference & Exhibition*, Extended Abstracts.

Mahrooqi, S., Al Rawahi, S., Yarubi, S., Al Abri, S., Yahyai, A., Al Jahdhami, M., Hunt, K. and Shorter, J. [2012] Land seismic low frequencies: Acquisition, processing and full wave inversion of 1.5 - 86 Hz. *82nd SEG Annual International Meeting*, Expanded Abstracts.

Masclet, S., Bardainne, T., Massart, V. and Prigent, H. [2019] Near-surface characterization in Southern Oman: Multi-Wave Inversion guided by Machine Learning. *81st EAGE Conference & Exhibition*, Extended Abstracts, Tu-R16-05.

Sternfels, R., Viguier, G., Gondoin, R. and Le Meur, D. [2015] Multidimensional simultaneous random plus erratic noise attenuation and interpolation for seismic data by joint low rank and sparse inversion. *Geophysics*, **80**(6), 129-141.

Stopin, A., Plessix, R.-E., Al Abri, S. [2014] Multiparameter waveform inversion of a large wide azimuth low-frequency land data set in Oman. *Geophysics*, **79**(3), WA67-WA7.
Wang, D., Chen, C., Zhuang, D., Mei, J. and Wang, P. [2021] Land FWI: challenges and possibilities. *82nd EAGE Conference & Exhibition*, Extended Abstracts
Wang, P., Zhang, Z., Mei, J., Lin, F. and Huang, R. [2019] Full-waveform inversion for salt: A coming of age. *The Leading Edge*, **38**(3), 304–213.
Zhang, Z., Wu, Z., Wei, Z., Mei, J., Huang, R. and Wang, P. [2020] FWI imaging: Full-wavefield imaging through full-waveform inversion. *90th SEG Annual International Meeting*, Expanded Abstracts, 656–660.
Zhao, J., Jin, H., Zhu, Y., El-Taha, Y. C. and Clow F. [2018] Vibroseis ultra high productivity blended acquisition: Field trial and full-scale implementation in Oman. *88th SEG Annual International Meeting*, Expanded Abstracts, 150–153.

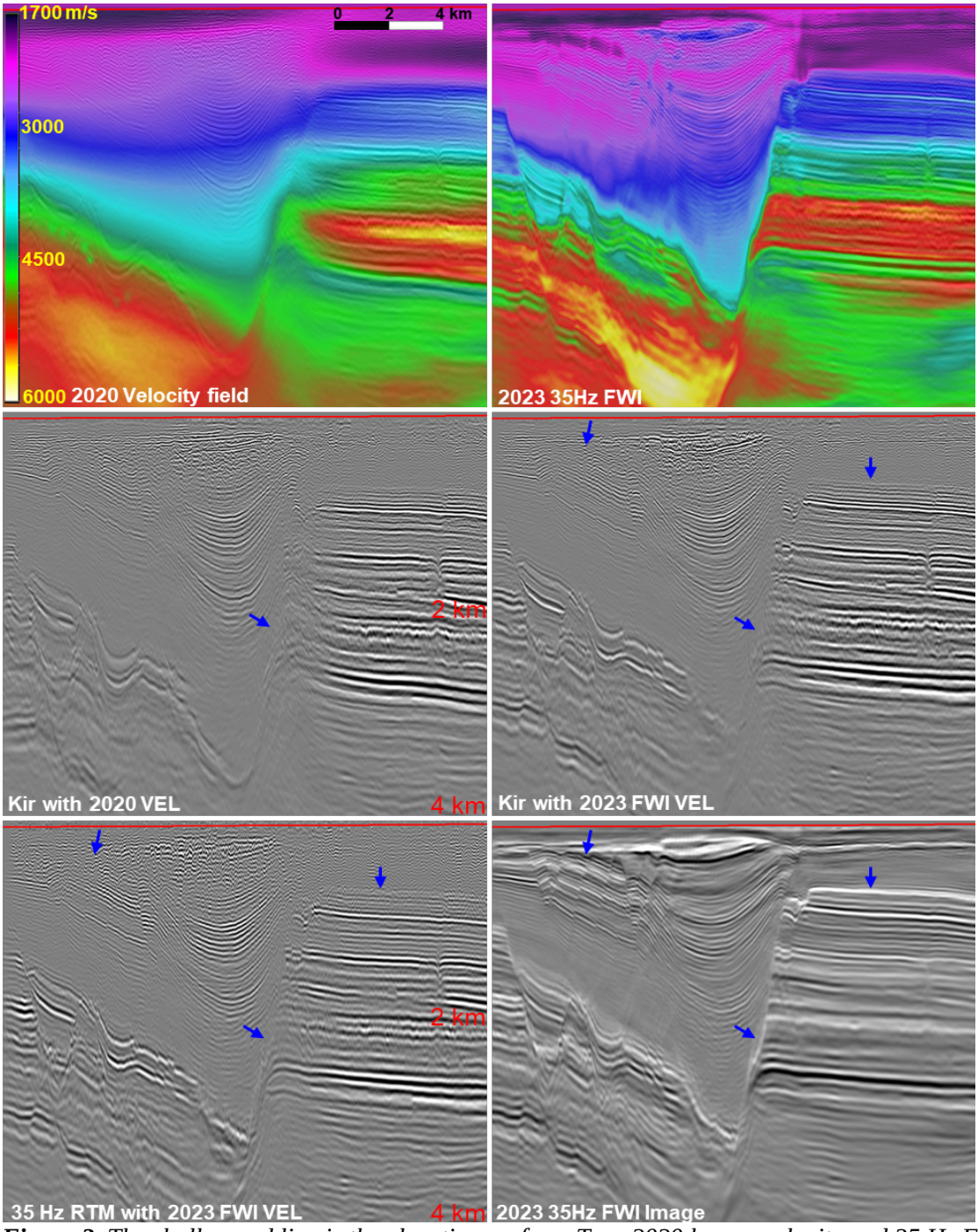

Figure 3. *The shallow red line is the elevation surface. Top: 2020 legacy velocity and 35 Hz FWI velocity. Middle: Kirchhoff PSDM with legacy velocity and FWI velocity. Bottom:35 Hz RTM with FWI velocity and 35 Hz FWI Image.*